Korzhuev M.A.

SOME BOTTLENECKS IN THE VEHICULAR THERMOELECTRIC GENERATORS AND A SEARCH FOR NEW MATERIALS TO ELIMINATE THEM

Korzhuev M.A., Granatkina Yu.V.
(*A.A. Baikov Institute of Metallurgy and Material Science of RAS, Laboratory of Semiconductor, 49, Leninskiy Ave., Moscow, 119991, Russian*)

Granatkina Yu.V.

• *We consider the impact of a thermoelectric generator (TEG) mounted on the exhaust pipe (EP) on the overall efficiency of a car. It is shown that the TEG has a mass factor considerably high ($m_{TEG} / m_{Car} \sim 0.01$, here m_{TEG} and m_{Car} are masses of the TEG and car, respectively), so mounting the TEG leads to additional losses in the motion of a car, comparable in size to the net electric power received from TEG ($W_{loss} \sim W_e \sim 0.2$ kW). Besides, the attached TEG comes into the conflict with the internal combustion engine (ICE) because of a competition of the two thermal machines for the thermal flows in the system (ICE + TEG). Since the efficiency of a thermoelectric generator is low (typically < 5%) a large amount of heat must be removed from the EP to the TEG. This heat comes to the cooling system (CS) of a car and can reduce the overall efficiency of the system (ICE+TEG). It is shown that the negative impact of TEG on the overall system can be reduced in the first place by increasing the figure of merit $Z = A/\kappa$ of thermoelectric materials, where $A = \alpha^2\sigma$ is the power factor, and α, σ, and κ are the Seebeck coefficient, electrical and thermal conductivity, respectively. It is shown that at Z = const and other things being equal, the most preferred thermoelectric materials for vehicular TEGs will be ones with the largest power factor A and, at the same time, with a low specific weight d.*

Introduction

The problem of fuel saving and a gain in overall power of a car ΔW makes the vehicular thermoelectric generator (TEG) relevant for waste heat recovery of the internal combustion engine (ICE) [1, 2]. Currently, prototypes of serial vehicular TEGs have been constructed with the net electrical power $W_e = 0.2 – 0.5$ kW making about 20 – 50 % of the electrical power necessary for vehicles [3 – 5]. Attempts at further increasing W_e encounter technical difficulties [2, 5]. Earlier we have assumed that these difficulties are also due to thermodynamic conflict of thermal machines (TM), the ICE and TEG, developing in the system (ICE + TEG) at mounting the TEG [6].

The present work is a continuation of research [6]; our purpose was to study in detail the conflict of TM developing in the system (ICE + TEG) with the TEG mounted on the exhaust pipe (EP) of a car. We consider some bottlenecks in mounting the TEG on the EP and a search for ways to eliminate them. It has been shown that the reason for conflict of TM is competition of the ICE and TEG for thermal flows in the system (ICE + TEG). The TEG is essentially weaker in comparison to the ICE ($W_e < 1$ kW << $W_{ICE} = 10^2 – 10^3$ kW) and of lower efficiency ($\eta_{TEG} \le 0.01 – 0.05 << \eta_{ICE} \le 0.4$) [7, 8]. For this reason the TEG takes away considerable thermal flows that disbalance the system (ICE + TEG) as a whole. As a result, with increasing $W_e > 0$ the conflict of TM develops in the system (ICE + TEG) that limits W_e TEG, ΔW and interferes with the work of the ICE.

When the TEG is mounted directly in the ICE, the conflict of TM is obvious [6]. In this case TM compete for the main thermal flow of burning fuel Q_0 and the general efficiency of the system drastically decreases ($\eta_{ICE + TEG} < \eta_{ICE}$), as part of the heat Q_0 is used by the less effective TM, the TEG [6]. When the TEG is mounted on the EP, the ICE and TEG compete for peripheral thermal flows

passing through the EP and vehicular cooling system (CS), as a result the conflict of the ICE and TEG decreases. The present work shows that in this case the conflict of the ICE and TEG can be further reduced and thus the TEG W_e and ΔW can be increased due to improving the TEG efficiency ($\eta_{TEG} > 0.1$). Accordingly, for this purpose new thermoelectric materials of enhanced figure of merit $Z = 0.005 – 0.01$ 1/K should be synthesized.

Currently, there is no consensus within the thermoelectric community on the prospects of using the vehicular TEG [1 – 5]. Some researchers are predicting widespread use of vehicular TEG in the near future, but the others believe that recovery of energy losses in cars will be produced by other, more effective methods [1, 9]. The results of the present study provide arguments in support of both views. The necessity of further research on the vehicular TEG with the use of new thermoelectric materials is confirmed [1, 4]. However, it is shown that in this case the expected values W_e and ΔW will be also considerably limited by the thermodynamic requirements existing in the system (ICE + TEG) [6].

1. General analysis

1.1. The TEG mass-factor

It is well known that the efficiency of the vehicular TEGs essentially depends on mass ratio of the TEG and vehicle [9]. For ships, diesel locomotives, etc. mounting the TEG does not cause essential relative increase in the weight of the system, but it not so for the cars and motorcycles [9]. Really, for power of burning fuel $Q_0 = 100$ kW, the mass of the TEG $m_{TEG} \sim 10$ kg, the mass of the car $m_{car} \sim 1000$ kg, and power of resistance to the motion $W^{RES} \sim (0.1 – 0.2)\ Q_0$ [7] one can get the increase in losses in motion of a car due to mounted TEG as $\Delta W_{loss} \sim 0.1 – 0.2$ kW which is close to a gain in the net electrical power of the TEG $W_e \sim 0.2$ kW [5]. An additional work required from the ICE to compensate the additional car load was estimated for a 1.5 l family car to be around 12 W/kg [4]. According to [4], employment of thermoelectric modules fabricated of low-density materials, such as magnesium silicide, can reduce considerably the energy losses of a car due to TEG weight penalty [4]. But the weight penalty is not a unique disadvantage of the vehicular TEGs [6].

1.2. System formation (ICE + TEG)

Besides, mounting the TEG in a car forms a complicated thermodynamic system (ICE + TEG) consisting of two diverse thermal machines, the ICE and TEG (Fig. 1) [7].

The ICE and TEG differ significantly in the way they are working as well as in their efficiency ($\eta_{TEG} << \eta_{ICE}$) (Table 1). As it is known, the ICE reaches its high efficiency $\eta^{ICE} \sim 0.4$ (Table 1) using the energy of fuel burning directly in the cylinders that needs no any additional heat exchanger at the hot side of the ICE [7]. In passing to the system (ICE + TEG) this advantage is lost as there is a need for additional heat exchangers at both on the hot and cold sides of the TEG [6, 7].

On the other hand, the TEG converts incoming thermal flow Q_0^{TEG} directly to the net electrical power by the Seebeck effect according to relation

$$W_e = \eta_{TEG} Q_0^{TEG}. \quad (1)$$

However, the efficiency of such conversion

$$\eta_{TEG} = 1 - Q_1^{TEG} / Q_0^{TEG} = W_e / Q_0^{TEG} = \left(\Delta T / T_1\right)\left(M - 1\right) / \left(M + T_0 / T_1\right) \quad (2)$$

is low enough (Table 1) (Here, Q_0 and Q_1 are incoming and outgoing heat flows; $\Delta T = (T_1 – T_0)$, T_1 and T_0 are temperatures of hot and cold joints of thermocouples; $M = (1 + Z\,(T_0 + T_1) / 2)^{1/2}$; $Z = \alpha^2 / ((\kappa_n / \sigma_n)^{1/2} + (\kappa_p / \sigma_p)^{1/2})^2$ is the figure of merit of modules; $\alpha = (\alpha_p – \alpha_n)$; $\alpha_{n,p}$, $\sigma_{n,p}$ and $\kappa_{n,p}$ are the Seebeck coefficient and the electric and thermal conductivities of the *n*- and *p*- legs, respectively.

Hereinafter subscripts 0 and 1 denote the incoming and outgoing heat fluxes) [8]. Therefore, even for production of a small amount of W_e the TEG needs a powerful incoming thermal flow Q_0^{TEG} as well as two heat exchangers on its inlet and outlet with a large throughput capacity ($\geq Q_0^{\mathrm{TEG}}$) [8].

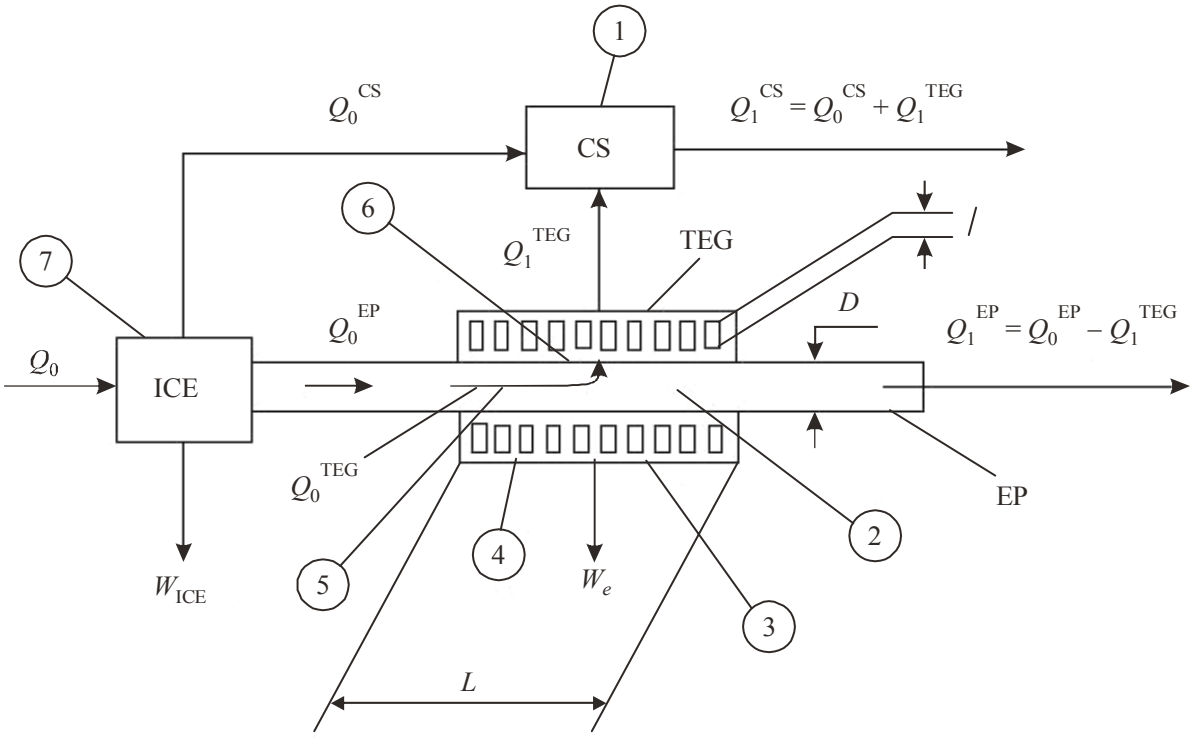

Fig. 1. Mounting the TEG on the EP in a car. System bottlenecks: 1 – CS overload by the TEG heat sink; 2 – fall of the EP temperature; 3 – low efficiency η^{TEG}; 4 – increased mass-factor of the TEG; 5 – little heat removal from the EP to the TEG; 6 – reduced temperature pressure of the TEG on the exhaust gas / EP interface; 7 – various interferences to the ICE work due to the TEG.

The mechanisms of heat transport from the heater to cooler in the ICE and TEG are also essentially different. In the ICE heat is transferred by hot exhaust gases through the exhaust pipes (EP), and partially through water and (or) air cooling system (CS) to atmosphere [7]. In the TEG, heat is transferred by the thermal conduction of solid-state legs and partially by the Peltier effect (~ 5 %) that is much less effective than the combined heat and mass transport in the tubes (Table 1) [8].

Accordingly, the effective thermal conductivity

$$K = Q_0 / \Delta T, \tag{3}$$

of the ICE and its peripheral parts (EP and CS) proves to be much higher than in the TEG. (Here Q_0 is incoming thermal flow, and ΔT is temperature difference) (Table 1) [9, 10]. Moreover, due to essentially different and incompatible mechanisms of heat transfer, only parallel joining the TEG to ICE or to its peripherals (EP and CS) is possible in the system (ICE + TEG) [6, 9]. But in parallel joining, the TEG removes from a heater only a part of thermal flow Q^H proportional to the TEG thermal conductivity [9, 10]

$$Q_0^{\mathrm{TEG}} = Q_0^H K^{\mathrm{TEG}} / \left(K^{\mathrm{TEG}} + K^H \right) < Q_0^H, \tag{4}$$

which decreases considerably the overall efficiency of heat conversion.

At mounting on the EP, the TEG joins to the main thermal flow Q_0 in parallel with the EP but in series with the ICE, owing to which the conflict of TM decreases. In this case, the ICE and TEG will

mainly compete for peripheral thermal flows passing through the EP and CS. Therefore, one can expect the increase in total efficiency of the system ($\eta_{ICE+TEG} > \eta_{ICE}$) if the TEG does not interfere with the work of the ICE [6].

1.3. Mounting the TEG on the EP

Figure 1 shows optimum mounting the TEG on the EP which assumes removal of heat Q_1^{TEG} into the existing (regular) CS of a car [1, 5]. This schematic is used by the majority of researchers as the main one, since the arrangement of additional own system of TEG water cooling (of mass at least 10 kg) leads to considerable TEG mass-factor increase and, accordingly, ΔW reduction [11]. Thus, using the regular vehicular CS for the TEG waste heat removal, the researchers limit the mass-factor of TEG, but are forced to overload the vehicular CS [6]. Besides, mounting the TEG on the EP causes a number of additional problems for heat exchange in the system (ICE + TEG). The basic of them are as follows: 1) to remove maximum power Q_0^{TEG} from the EP to the TEG, 2) to provide maximum temperature pressure (ΔT) on the TEG legs; 3) to provide removal of waste heat Q_1^{TEG} into the CS. These problems are solved using the respective heat exchangers with a high intrinsic figure of merit characterized by the Biot criterion

$$\mathrm{Bi} = \Delta T^{TEG} / \left(\Delta T_0 - \Delta T^{TEG}\right) = \Delta T^{TEG} / \left(\Delta T_1 + \Delta T_2\right). \quad (5)$$

Table 1

Some characteristics of the thermal machines and their parts within the system (ICE + TEG)[7, 8]

Thermal machine	Heat carriers	Efficiency, η	Incoming thermal flow, Q_0, kW	Working temperatures, $(T_1 - T_2)$, K	Temperature difference, ΔT, K	Effective heat conduction, $K = Q_0/\Delta T$, W / K	Output of the TEG W_e^{max}, kW
ICE	Exhaust gases	0.4	100	2500 – 1100	1400	71	
EP	Exhaust gases	–	30	900 – 450	650	66	
CS	Water and (or) air fluxes	–	30	373 – 323	50	600	
TEG:						28**	
In the ICE	Phonons and electrons	0.1*	< 28	2500 – 373	2127		< 28
On the EP		0.05*	< 5	900 – 373	527		< 0.45
On the CS		0.01*	< 1.3	373 – 323	50		< 0.01

*Figure of merit $ZT = 1$ (Bi_2Te_3), **Length of legs $l = 0.01$ m.

Here ΔT_0 and ΔT^{TEG} are the temperature difference applied at heat exchanger inlet and the real temperature difference along the legs, ΔT_1 and ΔT_2 are losses of temperature pressure in the cold and hot heat exchangers [9, 10]. Usually criterion Bi of 15 – 20 is considered as the optimum for the TEG, but for the vehicular TEG such Bi values seem unobtainable because of the generally large transient resistance of the exhaust gas / EP interface [10, 11].

1.4. Math approach and models for calculations

It is well known that calculation of a car is a complicated multivariable math problem solved only approximately [7]. With the TEG mounted on the EP, calculation of system (ICE + TEG) is further complicated due to arising two additional small parameters, W_e and $\Delta W \le W_e$. One can easily make certain that parameters W_e и ΔW are small by estimating the ratio $W_e / Q_0 \sim 0.2$ kW / 500 kW ~ 0.04 % [6] based on the experimental data obtained for car BMW 535i ($Q_0 \sim 500$ kW) [5]. Therefore, direct "first-principles" calculations of system (ICE + TEG) seem impossible, just as the exact experimental determination of ΔW value. Fortunately, the W_e value of the TEG can be exactly measured experimentally using the ammeter and voltmeter method and then used in the calculations as a fitting parameter with a well-known range of values.

In the present work we have made approximate thermal calculations of the system (ICE + TEG) to get a correct sign for ΔW and an approximate estimation of W_e value. As the input data, the tabulated data with different characteristics of cars [7] and materials were used [12]. The basic of them were: power released by burning fuel $Q_0 = 100$ kW ("city" car VAZ-2101 with engine volume 1.3 L and engine power $W_{ICE} \approx 54$ h.p.), $\eta_{ICE} = W_{ICE}/Q_0 = 0.4$, $Q_0^{CS} = Q_0^{EP} = 0.3Q_0$ and a number of characteristic temperatures of different car components (Table 1). The input data for thermal conductivities of the materials were $\kappa = 0.025$, 0.015, and 0.005 W/cm·K corresponding to crystals *PbTe*, Bi_2Te_3, and "phonon glasses". The efficiency values for TEG were $\eta_{TEG} = 0.03$, 0.05, and 0.1, corresponding to serial industrial, the best laboratory and perspective modules, respectively.

For calculations we used the standard layered model of the TEG [11], which has been extremely simplified (Fig. 2). Instead of the thermoelectric module inside the TEG with a complicated internal structure (1, Fig. 2) we used a continuous thermoelectric medium (2). In the calculation of parasitic thermal resistance we considered: (*a*) – adsorbed gas layer on the inner surface of the EP; (*b*) – EP body (*Fe*); (*c*) – *Fe* / TEG interface; (*d*) – TEG legs; (*e*) – TEG / *Al* interface; (*f*) – radiator (*Al*); (*j*) – radiator / coolant interface. Layers *a*, *b*, *d*, *f*, *j* were continuous, but layers *c* and *e* discrete, the last modeling the contact resistance of the legs (3, Fig. 2). Basic thicknesses of layers were *h*, *m*: *a* – 0.0001; *b* – 0.002; *c* – 0.001; *d* – 0.01; *e* – 0.001; *f* – 0.002; *j* – 0.001, that has been chosen taking into account the extensive experience of TEG design reported in the literature [10, 11]. The thickness of absorbed gas layer on the EP was taken to be equal to its average roughness *r* [11]. The latter was specified experimentally ($r \approx 0.0001$ m) using some fragments of a worked-out EP (Fig. 3). Partial heat resistance of continuous layers *a*, *b*, *d*, *f*, and *j* was counted by formula $R^T = h/\kappa S$ (Here κ is the thermal conductivity of materials, *h* and *S* are the thickness of layer and its area). Contact resistance of the legs (*c*, *e*, Fig. 2) was estimated by the same formula neglecting the metal contribution. The effective value of contact thickness was defined as $h^* \approx 10r$, where $r = 0.0001$ m is the roughness of the legs. Thus, the discrete layers (*c* and *e*, Fig. 2) were considered as the continuous thermoelectric medium of increased thickness [11]. In calculation of the TEG (Table 1), we used the length $L = 0.6$ m and the internal diameter $D = 0.05$ m for modules, and the length $l = 0.0001$ to 0.2 m for the legs (Fig. 1).

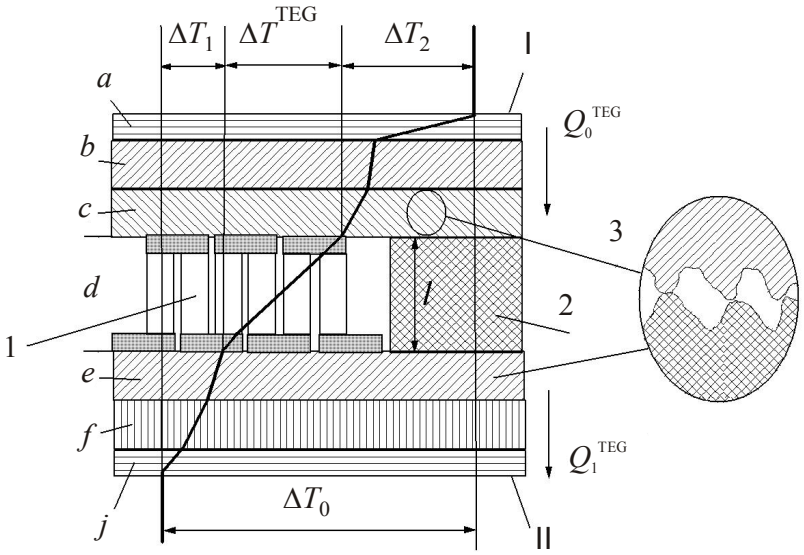

Fig. 2. Schematic of temperature distribution along the TEG cross-section. Sections: a – inner gas layer on the EP surface; b – EP body (Fe); c – Fe / TEG interface; d – TEG legs; e – TEG / Al interface; f – radiator (Al); j – radiator / coolant interface. I – hot side; II – cold side; 1 and 2 is thermocouple battery and its model; 3 is the model of TEG leg interface.

Thermal circuits of the vehicular TEG were approximately calculated in a manner similar to electrical chains. The Ohm's law $I = U / R$ and Kirchhoff's rule ($\Sigma I = 0$ for any point of a chain) were used as calculation formulae under the replacement $I \leftrightarrow Q$, $U \leftrightarrow \Delta T$, $R \leftrightarrow R^{T}$ (Here, I and Q are the electrical current and the heat flow, U and ΔT are the voltage and the temperature difference, R and R^T are the electrical and thermal resistances, $Q^{TEG} = Q^{EP}$. K^{TEG} / K, $Q^{EP'} = Q_0^{EP}$. K^{EP} / K, and $K = K^{EP} + K^{TEG}$ is the total thermal conductivity of the system (EP + TEG).

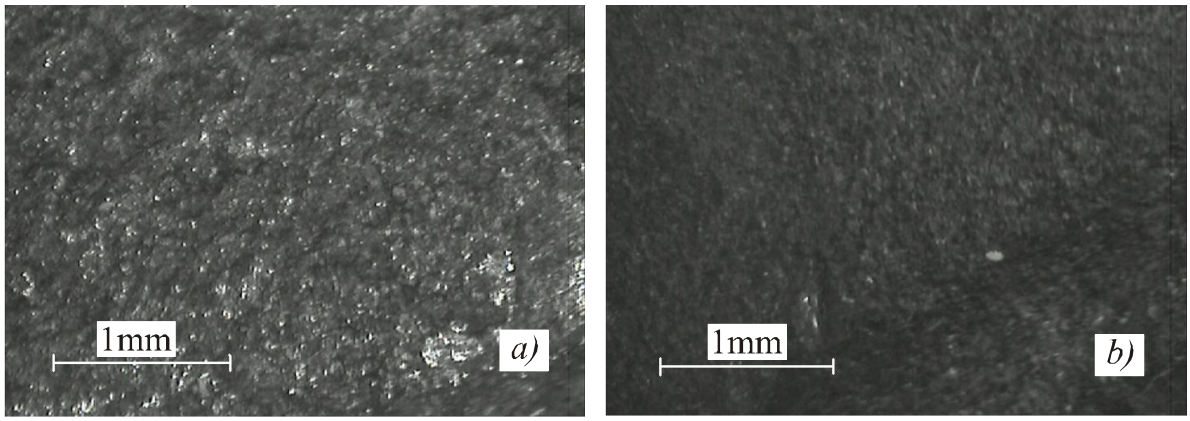

Fig. 3. The internal surface of EP that worked for 3 years in a 60 h.p. car (a, b). The maximum operating temperature T_{max}, K: (a) – 800; (b) – < 600. Surface kind: (a) – polished with hot gases; (b) – covered with a soot deposit (coke).

Fig. 4 shows the analog circuit model of heat flow in the system (EP + TEG) used for calculations. The partial temperature differences in the circuit $\Delta T_i = \Delta T \cdot R_i^T / R^T$ were calculated using total temperature difference $\Delta T = \Sigma_i \Delta T_i$ (Here $R^T = \Sigma_i R_i^T$ and R_i^T are total and partial heat resistances respectively). The effective thermal resistance of various components of the car was determined by the ratio $R_i^T = \Delta T_i / Q_i$ (Here Q_i is the passing heat flow, and ΔT_i is the corresponding temperature difference).

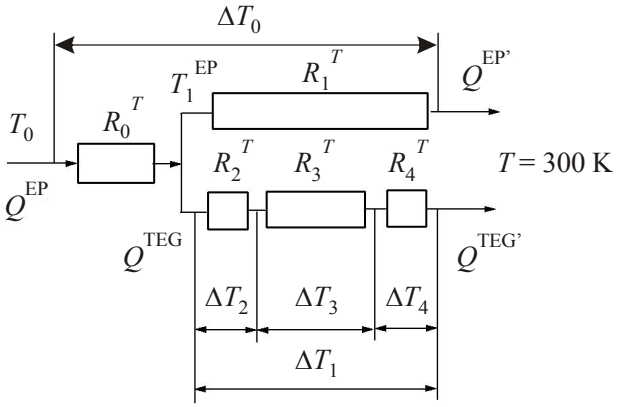

Fig. 4. Analog circuit of heat flow in the system (EP + TEG). Heat resistance of sections: R_0^T – EP beginning; R_1^T – EP end; R_3^T – the TEG; R_2^T and R_4^T – parasitic resistance at the interface of the heat exchangers.

2. Calculation results

2.1. System disbalance (ICE + TEG)

Some characteristics of the TM and their components calculated for the total power of burning fuel $Q_0 = 100$ kW are presented in the Table 1. Table 1 shows that heat conductivity (6) of various parts of the car follows a parity $K^{CS} < K^{ICE} < K^{EP} < K^{TEG}$. Consequently, the incoming heat flow Q_0^{TEG} TEG and W_e is essentially limited with any arrangement of the TEG in a car. In particular, with the TEG mounted on the EP, we get maximum $Q_0^{TEG} \approx 1/3 Q_0^{EP}$ and $W_e^{max} \approx 0.45$ kW at the best.

Fig. 5 shows a change of heat balance in the system (ICE + TEG) versus the electrical power W_e of the TEG. Curves (Fig. 5) were calculated by formula (1) for $\eta_{TEG} = 0.05$ using the equation of power balance of systems $Q_0 = W_{ICE} + Q_0^{CS} + Q_0^{EP} + W_e$. When calculating the curves (Fig. 5) we assumed that installation of the TEG on the EP does not decrease the W_{ICE} of the ICE.

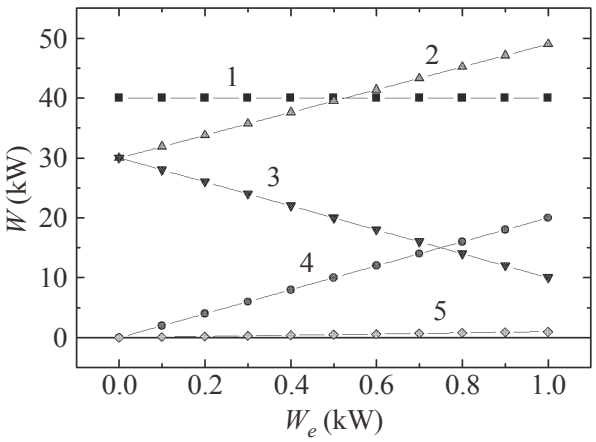

Fig. 5. Redistribution of energy flows in the system (ICE + TEG) versus net electrical power W_e with the TEG mounted on the EP. 1 – W_{ICE}; 2 – Q^{CS}; 3 – Q^{EP}; 4 – Q^{TEG}, 5 – ΔW. ($\eta_{TEG} = 0.05$).

According to Fig. 5, increase in the W_e causes dramatic changes in the system (ICE + TEG). Namely, the heat flows Q_0^{TEG} and Q_0^{CS} through the TEG and CS are both increased by 20 kW (curves 4 and 2), but Q_1^{EP} through the EP is decreased by 20 kW (curve 3). Thus, the total gain in the net power $\Delta W = \Delta W_e$ (curve 5, Fig. 5) proves to be much smaller than the total redistribution of heat flows

in the system (curve 2 to 4). Therefore, the TEG will cause a significant change in thermal conditions of the EP and CS (Fig. 6, 7).

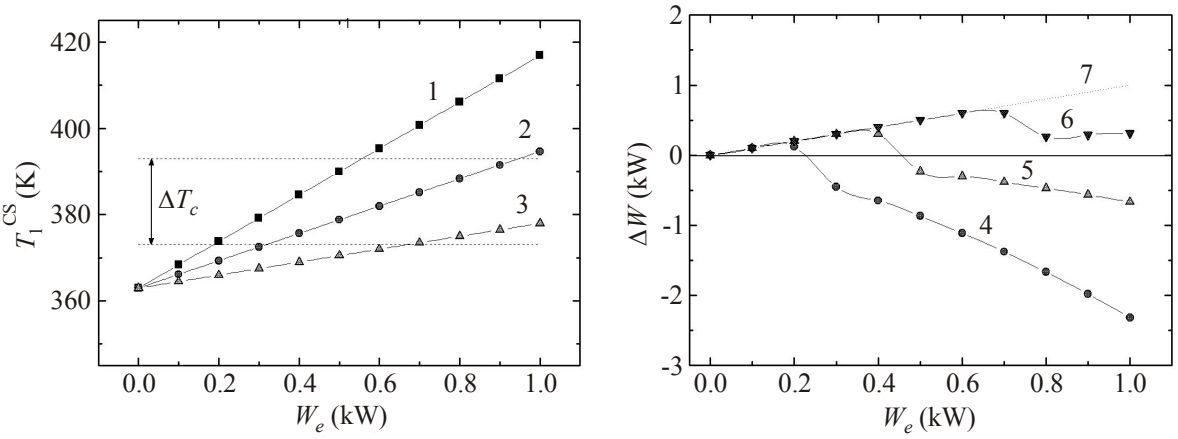

Fig. 6. Increase in temperature T_1^{CS} of the hot side of the CS (a) and net power gain ΔW of the system (ICE + TEG) (b) versus the net electrical power W_e of the TEG. 4 – 6 – $\Delta W = W_e - W_c^{CS'}$; 7 – $\Delta W = W_e$. η_{TEG}*: 1, 4 – 0.03; 2, 5 – 0.05; 3, 6 – 0.1. The arrows show the water boiling range ΔT_c in the CS.*

Fig. 6 *a* shows increase in temperature T_1^{CS} at the hot side CS due to the TEG heat removal. Calculations T_1^{CS} were made under formula $T_1^{CS} = T_0^{CS} + Q_1^{CS} / K^{CS}$, where $T_0^{CS} = 313$ K is the basic temperature of a cold side the CS, $Q_1^{CS} = Q_0^{CS} + Q_1^{TEG}$ is the resulting heat flow CS (Fig. 1), and $K^{CS} = 0.6$ kW/K is the effective heat conduction of the CS (Table 1). From Fig. 6 *a* it is seen that with the growth W_e, and depending on η_{TEG}, the temperature T_1^{CS} will increase reaching an interval of boiling water in radiator $T_0 = 373 – 393$ K. Therefore, at supplying no additional expenses of energy to compulsory cooling system ΔW_c^{CS}, the water in the CS begin to boil and the engine will stop. On the other hand, at the necessary increase of initial W_c^{CS} the gain in ΔW may be questionable. Fig. 6 *b* shows the total gain in the net power ΔW in the system (ICE + TEG) due to growth of W_e accompanied by the growth of expenses for compulsory cooling to $W_c^{CS'} = W_c^{CS} + \Delta W_c^{CS}$. The size of $W_c^{CS'}$ was calculated using the conditions of $W_c^{CS} = 1$ kW (0.033 Q^{CS}), $W_c^{CS'} = W_c^{CS} (Q^{CS'} / Q^{CS})^2$. A quadratic approach for calculations $W_c^{CS'}$ corresponded to boiling water which breaks heat transfer processes in the CS and demands additional to linear expenses of energy to prevent stop the ICE.

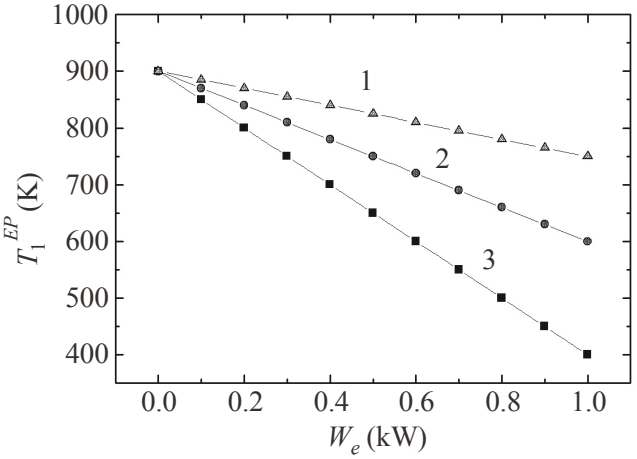

Fig. 7. Reduction of the EP hot side temperature T_1^{EP} versus the TEG net electrical power W_e. η_{TEG}*: 1 – 0.03; 2 – 0.05; 3 – 0.1.*

According to calculations (Fig. 6 *b*), it always exists a narrow range of W_e TEG near zero, where waste heat recovery in the system (ICE + TEG) may be possible ($\Delta W > 0$) using reserves the regular CS of a car [2]. On the contrary, for enough big W_e the gain in ΔW is not observed at all (curves 1, 2), or it is significantly reduced due to the growth of ΔW_c^{CS} (curve 4). For this reason, a real waste heat recovery ($\Delta W > 0$) in a car needs a TEG with the increased efficiency $\eta_{TEG} > 0.1$.

Fig. 7 shows a decrease in the temperature T_1^{EP} of the EP hot side versus the net electrical power W_e due to heat removal by TEG. Calculations of T_1^{CS} were made by formula $T_1^{EP} = T_0^{EP} + Q_1^{EP} / K^{EP}$, where $T_0^{EP} = 450$ K is the basic temperature of the EP cold side, $Q_1^{EP} = Q_0^{EP} - Q_0^{TEG}$ is the resulting heat flow of the EP (Fig. 1), and $K^{EP} = 66$ W/K is the effective heat conduction of the EP (Table 1). In turn, a decrease in the EP hot side temperature reduces the Carnot factor ($\Delta T / T$) of the TEG thus decreasing η_{TEG} and W_e [7]. On the other hand, the respective decrease in temperature of the exhaust gases reduces their viscosity χ (from ~ 35 Pa·s at 800 K to ~ 22 Pa·s at 400 K) [12] which may reduce a little the EP counter pressure, thus reducing the losses in the system.

2.2. Temperature pressure along the legs

Fig. 8 and 9 show the temperature distribution along the TEG and the incoming heat flow Q_0^{TEG} through the TEG for the case of air (*A*, curves 1 – 3) and water (*B*, curves 4 – 6) cooled modules.

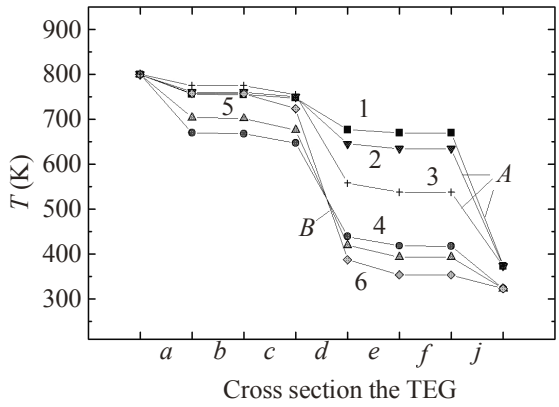

Fig. 8. Distribution of the temperature T along the TEG cross-section for air (A) and water-cooled modules (B). The sections are specified in Fig. 2. The height of sections h, m: a – 0.0001; b – 0.002; c – 0.001; d – 0.01; e – 0.001; f – 0.002; j – 0.001. Thermal conductivity of the legs κ, W / (cm·K): 1, 4 – 0.025; 2, 5 – 0.015; 3, 6 – 0.005. Total criterion Bi: 1 – 0.16; 2 – 0.26; 3 – 0.65; 4 – 0.71; 5 – 1.06; 6 – 2.05.

Calculations were carried out for the case of idling TEG in the range of temperatures $T = 300 – 800$ K using a model of TEG (Fig. 2) and the analogue circuit of heat flow (Fig. 4). Calculations of parasitic thermal resistance R_2^T of the hot side of TEG (Fig. 4) were made with account of gas layer on the EP surface, EP body and *Fe* / TEG interface. (Sections *a* to *c*, Fig. 8). Accordingly, calculations of parasitic thermal resistance R_4^T of the cold side of TEG (Fig. 4) were made with account of TEG / *Al* interface, radiator/coolant interface and thermal resistance of radiator (*Al*) (Section *a* to *c*, Fig. 8). According to Fig. 8, the parasitic thermal resistances R_2^T and R_4^T (Fig. 4) contribute considerably to temperature distribution along the TEG. Among them, the most essential is the spurious thermal resistance of gas/solid interface in heat exchangers [7, 9]. Therefore, the values of total criterion Biot $Bi = 0.16 – 0.65$ and $Bi = 0.71 – 2.05$ calculated for air and water cooled modules in all cases proved to be rather low (Fig. 8). As long as air cooled modules have undesirable gas/solid interfaces at two points at once, on the hot and cold sides, their incoming heat flow Q_0^{TEG} is twice reduced (curves *B* to *A*, Fig. 9).

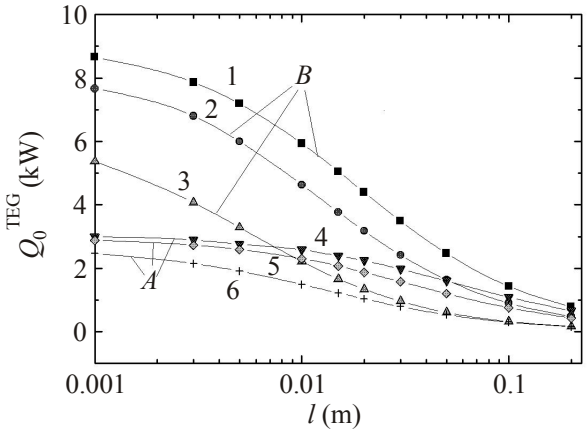

Fig. 9. The incoming heat flow Q_0^{TEG} of TEG versus the leg length l for air (A) and water-cooled modules (B). Thermal conductivity of legs κ*, W / (cm·K): 1, 4 – 0.025; 2, 5 – 0.015; 3, 6 – 0.005.*

For this reason, the air-cooled modules with a sufficiently large net electrical power W_e of TEG are difficult to construct. It is only water-cooling that makes significant temperature difference in modules and considerable heat flows towards the TEG (*B*, Fig. 8). Nevertheless, even in this case because of the low figure of merit of the hot heat exchanger, criterion Bi of the vehicular TEG is essentially reduced as compared to the standard ones (Bi = 15 – 20) [10]. Therefore, the parasitic resistance R_2^T (Fig. 4) at the exhaust gas/ EP interface reduces considerably the temperature difference ΔT along the TEG, as well as W_e. Moreover, the decrease in temperature on the EP hot side (Fig. 7) may result in additional increase of R_2^T due to intensive deposit of soot (coke) on the internal surface of the EP (Fig. 3 *b*) [11]. Consequently, in the real practice one will obtain no more than ~ 50 – 70 % of the TEG W_e primarily expected [10, 11].

2.3. Promising materials for the vehicular TEGs

Fig. 10 shows calculations of expected maximum net electrical power W_e^{max} TEG versus the length of legs. At calculation of W_e^{max} we used formulae (1) and (2) and the calculated results of incoming heat flow Q_0^{TEG} (Fig.9), and temperature pressure on the legs ΔT^{TEG} (Fig. 8). In accordance with this calculations, the maximum W_e^{max} TEG for water cooled modules is ~ 0.5 kW and ~ 0.9 kW for the figure of merit modules Z = 0.003 1/K and 0.01 1/K, respectively (Fig. 10).

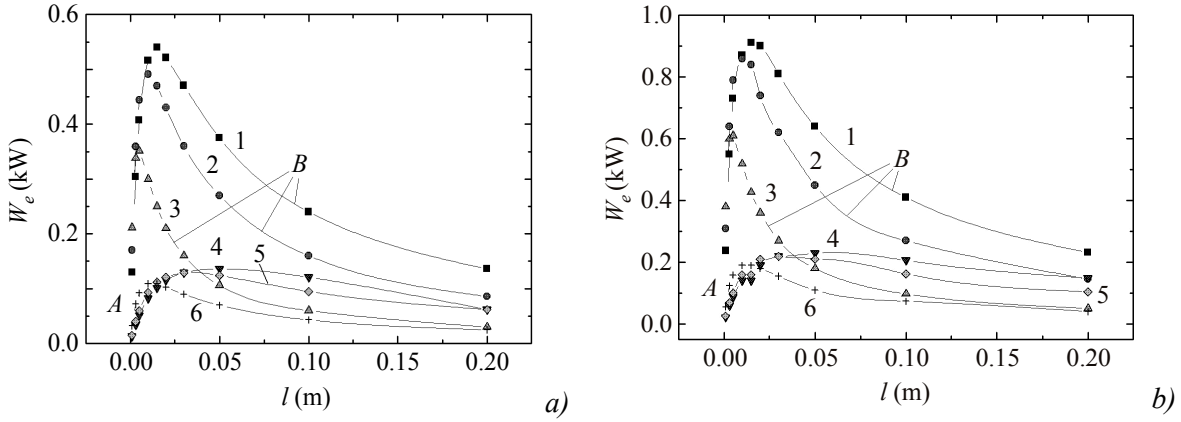

Fig. 10. The net electrical power W_e of TEG versus the length of leg l for air (A) and water-cooled modules (B) (a, b). Thermal conductivity of the legs κ*, W / (cm·K): 1, 4 – 0.025; 2, 5 – 0.015; 3, 6 – 0.005. Figure of merit of modules, Z, 1/K: (a) – 0.003; (b) – 0.01.*

According to (Fig. 10), the thermoelectric materials with a low thermal conductivity κ similar to phonon glasses [13] have a reduced optimum length of legs which is important for saving expensive and scarce thermoelectric materials and for decreasing the TEG mass-factor [10, 11]. At the same time, we find that for $Z = \alpha^2\sigma / \kappa = \text{const}$, other things being equal, the materials with a higher power factor $A = \alpha^2\sigma$ will be more preferable for vehicular TEG than the phonon glasses with a low κ (curve 3 to 1, and 6 to 4, Fig. 10) [8]. This result has a simple physical meaning which is explained in Fig. 11.

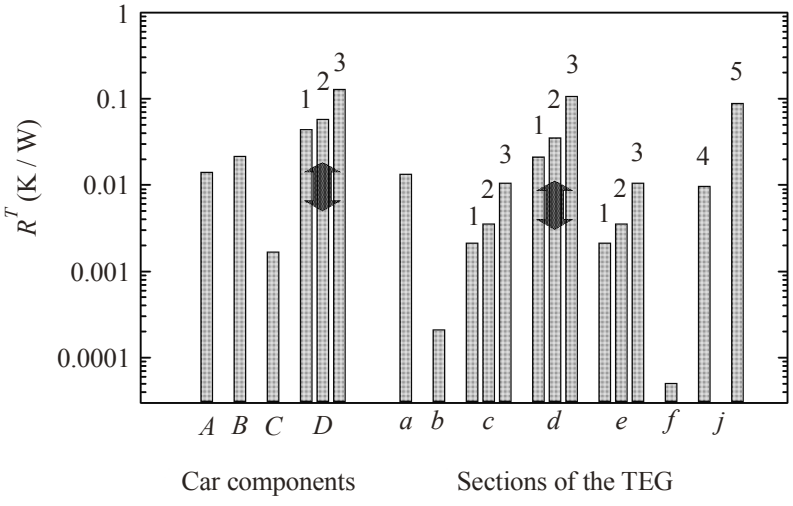

Fig. 11. Relative thermal resistance R^T of car components (A – C) and TEG sections (a – j).
Car components: A – ICE; B – EP; C – CS; D – TEG. TEG sections: a – inner gas layer on the EP surface; b – EP body (Fe); c – Fe / TEG interface ; d – TEG legs; e – TEG / A interface l; f – the radiator (Al); j – radiator / coolant interface. Thermal conductivity of the legs κ*, W / (cm·K): 1 – 0.025; 2 – 0.015; 3 – 0.005. Cooling of the TEG: 4, D – water; 5 – air.*
Arrows show parameters varying with the length of the legs l.

Fig. 11 shows relative thermal resistance $R^T = 1/K$ of various car components and TEG sections. The vehicular TEGs carry out simultaneously two functions: 1) heat transfer from heater to cooler and 2) heat conversion into electricity [8, 10]. To perform the first function, the modules should have relatively high heat conduction $K = 1/R^T$ (*D*, Fig. 11), but for the second function they should have a low heat conductivity κ of legs ($Z = \alpha^2\sigma / \kappa$). Usually this contradiction is removed by reducing the length of legs *l*, thus R^T of the legs (*d*) and so total R^T of modules (*D*) is decreased (arrows, Fig. 11) [10, 11]. But the reduction of *l* has a limit due to the unvaried boundary resistances (*a* to *c*, and *e* to *j*, Fig. 11) decreasing the temperature pressure on the legs for smaller *l* [8, 10, 11]. In the vehicular TEGs due to the increased parasitic heat resistance R_2^T (*a*, Fig. 11), the total boundary resistance is particularly high, therefore the optimum height of TEG legs appears big enough (l ~ 0.01 – 0.02 m) (Fig. 10) [10, 11]. According to our calculations, a considerable contribution to total boundary resistance of the TEG is brought also by the contact resistance of materials of legs inversely proportional to the specific heat conductivity κ of thermoelectric materials (*c* and *e*, Fig. 11). Therefore, at an identical surface roughness *r* the contact resistance of the phonon glasses appears essentially big (*c* and *e*, 1 to 3, Fig. 11). These contact resistance do not change with *l*, thus for smaller *l* their contribution appears essential. We have found out that exactly these contact resistances are responsible for the decrease in $W_e^{\max}$ of the phonon glasses in comparison to the materials of higher power factor *A* (Fig. 10). In our opinion, the increased contact resistance can essentially limit the use of phonon glasses in vehicular TEGs [11]. Nevertheless, recently, a simultaneous increase of heat

conduction K and figure of merit Z modules was observed for graded legs that may be especially useful for vehicular TEGs [14].

3. Discussion

In the present paper we have considered the problem of vehicular TEGs with regard to conflict of thermal machines (TM), the ICE and TEG. The ICE and TEG are the diverse thermal machines, therefore, mounting the TEG in a car brings about a thermodynamic conflict with the ICE due to competition of the TM for heat flows in the system (ICE + TEG) [6]. With the TEG directly mounted in the ICE, the TM compete for the power of burning fuel Q_0. In this case, the conflict quickly develops with the growth of W_e which decreases drastically the overall system efficiency ($\eta_{ICE+TEG} < \eta_{ICE}$) [6]. With the TEG mounted on the EP, the TM compete for peripheral heat flows passing through the EP and CS, therefore the conflict can be reduced by increasing η_{TEG} (Fig. 6 – 10).

In the present work it is shown that with the arrangement of the TEG on the EP there is a narrow range of W_e TEG, where waste heat recovery in the system (ICE+TEG) may be possible ($\eta_{ICE+TEG} > \eta_{ICE}$). This conclusion was obtained for an ideal case, when the TEG does not interfere with the ICE and the negative mass factor of installed TEG is not taken into account. In practice, mounting the TEG on the EP will create additional load on the car and may reduce its total efficiency. Besides, because of the EP temperature reduction, the TEG can violate the turbo-resonant boost in the ICE, regulating processes of fuel intake into cylinders and removal of waste gas from them [6]. These two factors may lower the net power of engine W_{ICE} for 5 % and more [6], however they may be eliminated or reduced by technical methods.

On the other hand, with the arrangement of the TEG on the EP the conflict in the system (ICE + TEG) will further develop due to: 1) different mechanisms of the ICE and TEG; 2) mismatched efficiencies of the ICE and TEG ($\eta_{TEG} << \eta_{ICE}$); 3) mismatched thermal resistances of the TEG and EP (Table 1). Numbers in circles (Fig. 1) show the main bottlenecks of vehicular TEGs resulted from the diversity of the TEG and ICE and a fatal conflict between them. These bottlenecks are: 1) overloading the car CS by the TEG waste heat; 2) drop of EP temperature; 3) low values of η^{TEG}; 4) increased TEG mass-factor; 5) too low heat removal from the EP to the TEG; 6) decrease of temperature pressure on the TEG at the exhaust gas / EP interface; 7 – various interferences to the ICE work due to the TEG [15].

Therefore, we seek for ways of eliminating some bottlenecks of the TEGs by reducing the conflict in the system (ICE + TEG). There are two ways for reducing the conflict between the TEG and ICE in a car. The first way is to decrease the ratio W_e / Q_0 by using more powerful cars. The second way assumes TEG efficiency increase up to $\eta_{TEG} \geq 0.1$ using new materials with a higher figure of merit Z. According to our estimates, for $Z = 0.005$ 1/K one can get $W_e \sim 0.8$ kW ($Q_0 = 100$ kW) and in this case waste heat recovery in the system becomes possible ($\eta_{ICE+TEG} > \eta_{ICE}$). The most preferred thermoelectric materials for the vehicular TEG are those with higher power factor $A = \alpha^2\sigma$ and inhomogeneous distribution of current carrier concentration along the length of legs (segmented, graded, etc.) [14].

4. Conclusion

Mounting the TEG in a car due to high mass- factor of the TEG ($m_{TEG} / m_{Car} \sim 0.01$) leads to additional power losses in motion comparable on size with the useful electric power received from the TEG ($W_{loss} \sim W_e \sim 0.2$ kW). Besides, the attached TEG comes into a fatal conflict with the internal combustion engine (ICE) of a car because of competition between thermal machines for energy flows in the system (ICE + TEG). As a result, the TEG interferes with the work of the ICE, so total efficiency of the system (ICE + TEG) can be further reduced. The negative impact of TEG on the

overall system (ICE + TEG) can be lowered in the first place by increasing the figure of merit Z of thermoelectric materials as well as by using the materials of low specific weight.

Acknowledgment. We thank Dr. Kiseleva N.N. for helpful advice on the thermodynamics of irreversible processes.

References

1. Vining C.B. The Limited Role for Thermoelectrics in Climate Crisis // J. Thermoelectricity. 2008. – №4. – P. 7 – 19.
2. Saqr K.M., Mansour M.K., Musa M.N. Thermal Design of Automobile Exhaust-based Thermoelectric Generators: Objectivities and Challenges // J. Thermoelectricity. 2008. – № 1. – P. 59 – 66.
3. Anatychuk L.I., Luste O.J., and Kuz R.V. Theoretical and Experimental Study of Thermoelectric Generators for Vehicles // J. Electronic Materials. 2011. – V. 40. – № 5. – P. 1326 – 1331.
4. Rowe D.M., Smith J., Thomas G., Min G. Weight Penalty Incurred in Thermoelectric Recovery of Automobile Exhaust Heat // J. Electronic Materials. 2011. – V. 40. – № 5. – P.784 – 788.
5. Lieb J., Neugebauer S., Eger A., Linde M., Masar B., Stűtz W. The Thermoelectric Generator from BMW is Making Use of Waste Heat // MTZ. 2009. – V. 70. – № 4. – P. 4 – 11.
6. Korzhuev M.A., Katin I.V. On the Placement of Thermoelectric Generators in Automobiles // J. Electronic Materials. 2010. – V. 39. – № 9. – P. 1390 – 1394.
7. Kirillin V.A., Sychev V.V., Sheindlin A.V. Technical thermodynamics. Moscow: Energiya. – 1974. – 448 p.
8. Ioffe A.F. Semiconducting Thermoelements. Moscow-Leningrad: Izd. AN SSSR. – 1960. – 188 p.
9. Manasian Yu.G. Ship's thermoelectric devices and installations. Leningrad: Sudostroenie. – 1968 – 284 p.
10. Kotyrlo G.K., Lobunets Yu.N. Calculation and designing of thermoelectric generators and thermal pumps. Handbook. Kiev: Naukova Dumka. – 1980. – 328 p.
11. Lykov A.V. Heat and substance interchange. Handbook. Moscow: Energia. – 1972. – 560 p.
12. Physical Properties of Materials. Handbook. Ed: I.S. Grigoriev, E.Z. Meilikov. Moscow: Energoatomizdat. – 1991. – 1232 p.
13. Nolas G.S., Sharp J., Goldsmid H.J. Thermoelectrics. Basic Principles and New Materials Developments. Berlin, Heidelberg, N.Y.: Springer. – 2001. – 293 p.
14. Korzhuev M.A. Symmetry Analysis of Thermoelectric Energy Converters with Inhomogeneous Legs // J. Electronic Materials. 2010. – V. 39. – № 9. – P. 1381 – 1385.
15. Korzhuev M.A. Conflict between Internal Combustion Engine and Thermoelectric Generator during Waste Heat Recovery in Cars // Technical Physics Letters. 2011. V. 37. № 2. P. 151 – 153.

Submitted 01.06.2011.